Thermal effects on the switching kinetics of silver/manganite memristive systems

2014 J. Phys. D: Appl. Phys. 47 435304

(http://iopscience.iop.org/0022-3727/47/43/435304)

IOP Publishing Journal of Physics D: Applied Physics
J. Phys. D: Appl. Phys. **47** (2014) 435304 (5pp) doi:10.1088/0022-3727/47/43/435304

Thermal effects on the switching kinetics of silver/manganite memristive systems

P Stoliar[1,2], M J Sánchez[3,4], G A Patterson[5] and P I Fierens[4,5]

[1] ECyT, UNSAM, 1650 San Martín, Argentina
[2] CIC nanoGUNE, 20018 Donostia-San Sebastián, Basque Country, Spain
[3] Centro Atómico Bariloche and Instituto Balseiro, CNEA, 8400 Bariloche, Río Negro, Argentina
[4] Consejo Nacional de Investigaciones Científicas y Técnicas (CONICET), C1033AAJ Buenos Aires, Argentina
[5] Instituto Tecnológico de Buenos Aires (ITBA), C1106ACD Buenos Aires, Argentina

E-mail: submissions@iop.org

Received 16 July 2014, revised 29 August 2014
Accepted for publication 4 September 2014
Published 7 October 2014

Abstract
We investigate the switching kinetics of oxygen vacancy (Ov) diffusion in La(5/8-y)Pr(y) Ca(3/8)MnO(3)-Ag (LPCMO–Ag) memristive interfaces by performing experiments on the temperature dependence of the high resistance state under thermal cycling. Experimental results are well reproduced by numerical simulations based on thermally activated Ov diffusion processes and fundamental assumptions relying on a recent model proposed to explain bipolar resistive switching in manganite-based cells. The confident values obtained for activation energies and the diffusion coefficient associated to Ov dynamics constitute a validation test for both model predictions and Ov diffusion mechanisms in memristive interfaces.

Keywords: memristive, manganite, oxygen vacancy, memory

(Some figures may appear in colour only in the online journal)

1. Introduction

Resistive memories (ReRAMs) based on oxide's compounds are receiving a lot of attention in view of their potential use for the next generation of non-volatile memories. Its operation relies on the resistive switching (RS) effect, which is the change in resistance of the device between two different values, the high resistance state (HRS) and the low resistance state (LRS), by an appropriate electric stimulus [1, 2]. The transition from HRS to LRS is called a **set** while the opposite process is defined as **reset**.

A large variety of oxides have been explored for ReRAM applications, ranging from binary transition metal oxides [3–7] to complex ones—manganite and perovskite-like [8–14].

In the case of devices based on complex oxides, the emerged consensus points to voltage-driven ion migration toward the metal–electrode interfaces as the relevant mechanism controlling bipolar RS, i.e. the switching mode dependent on voltage polarity [2]. In particular, oxygen vacancies (Ovs) have been proposed as the active agents participating in the bipolar RS effect [15–19].

The introduction of dopants for the improvement of ReRAM has also been reported consistently. As an example, the efficiency of Ov migration by Nb doping $Ba_{0.7}Sr_{0.3}TiO_3$ (BST) thin films, was tested in [20]. As stated in that work, the distribution of defects is strongly related to the RS properties, assisting Ov migration and making the ReRAM operation more efficient.

Although the exact microscopic origin behind the RS effect remains elusive, a recent phenomenological model, named the **voltage enhanced oxygen vacancy** (VEOV) migration model [21], succeeded in reproducing many non trivial characteristics of bipolar resistive switching found in experiments with complex oxides [12, 13, 22]. The VEOV model incorporates as main ingredients:

- the drift/diffusion of Ov along highly resistive metal/oxide interfaces, where strong electric fields are developed;
- a linear relation between resistivity and Ov concentration;
- the main contribution to the resistance comes from the density of oxygen vacancies in a region near the electrodes.

Depending on the polarity of the electric field during a switching operation, vacancies may accumulate or void

nano-sized regions at the metal/electrodes interfaces, giving a place to the reset and set transitions, respectively. In spite of the success of the VEOV model in reproducing many experimental features of bipolar RS, the drift/diffusion of Ov has only been tested indirectly [12, 14].

The goal of the present work is to probe the switching kinetics proposed in the VEOV model, by studying the response of the switched high resistance state under thermal cycling in a manganite (LPCMO)–Ag device. Nian *et al* [15] studied the relaxation time of the HRS at a fixed temperature for different temperatures in samples of $Pr_{0.7}Ca_{0.3}MnO_3$. Assuming a linear relation between resistance and Ov density, they estimated, e.g. the activation energy of vacancy diffusion. In section 2, we not only reproduce the same type of measurements on samples of $La_{5/8-y}Pr_yCa_{3/8}MnO_3$, but we go a step further by varying sample temperature in a controlled manner during the experiments. We shall show that diffusion can be either activated by increasing temperature or 'frozen' by decreasing it.

In section 3 we put forth a simplified model of oxygen vacancy diffusion. As we shall show in section 4, our model fits experimental data quite well and allows us to extract confident values for the activation energy and diffusion coefficient associated to Ov dynamics. We close this manuscript with some conclusions in section 5.

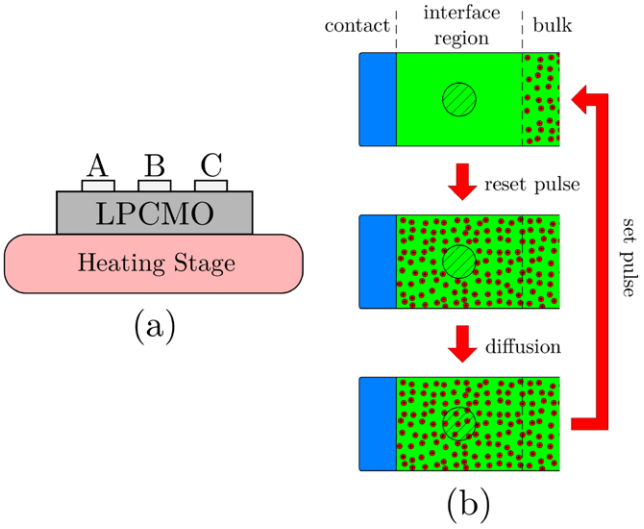

Figure 1. (a) Scheme of the experimental setup. (b) Model description and proposed mechanism described in the text. While the sample is in the LR state, Ov are mostly in the bulk. Under a reset pulse, the Ov move to the interface region and the HR state is attained. However, there is a region (shadow area in the figure) which still remains void of vacancies. When the pulse is switched off, the temperature activated diffusion process can further increase the interface resistance by the infilling of Ov in the previously void region.

2. Experimental results

We conducted experiments on two manganites $La_{5/8-y}Pr_yCa_{3/8}MnO_3$ (LPCMO)-based samples. Contacts were made by depositing drops of silver paint of 1–2 mm diameter over the LPCMO pellet. Sample fabrication and some of its characteristics were presented by Levy *et al* [23]. Moreover, the bipolar RS behaviour of this compound has been broadly studied [11–14, 21, 22, 24]. Each sample was coupled to a different heating stage (see figure 1) in order to perform two completely independent analyses in different laboratories. In setup #1 temperature was controlled by a LakeShore 331 Temperature Controller, having an error lower than 1 K. Setup #2 consisted of an *ad hoc* heating stage based on a Peltier cell controlled by an Arduino board.

The inset of figure 2 presents an example of the evolution of the resistance in setup #2 after setting the high resistance state at a fixed temperature (353 K). As it can be observed, resistance evolves in time even in the absence of an external stimulus. Indeed, based on the main assumptions of the VEOV model, we may hypothesize that, even after the reset pulse has been applied, oxygen vacancies continue diffusing into a region near the interface and, hence, resistance changes. In section 4 we shall come back to figure 2 and we shall estimate the activation energy of Ov diffusion by analysing the temporal evolution of resistance at constant temperature.

Figures 3–4 present results corresponding to more complex experiments where the temperature was continuously varied. The general procedure employed consisted on the application of a reset pulse at an initial temperature and then recording the resistance of a single interface—R_A corresponding to contact A in figure 1(*a*)—during several cyclic temperature sweeps. For each temperature, resistance was determined by applying a small bias current between terminals A and C and measuring the voltage drop between A and B.

In figure 3 we present results corresponding to setup #1. We swept the temperature from 323 K to 455 K with a rate of $\pm$ 10 K min^{-1}. Results are plotted on a semi-log scale versus $T^{-\frac{1}{4}}$. As it can be seen, during the last temperature cycle, resistance measurements appear to fall on a line. These results are consistent with the variable range-hopping (VRH) model [25]. Indeed, VRH postulates that the dependence of resistance with temperature is given by

$$R = R_0 \exp\left(\frac{T_0}{T}\right)^{\frac{1}{4}}, \tag{1}$$

where the characteristic temperature T_0 depends on the localization of the charge carriers and R_0 is a scaling factor. Although the temperature range of our experiments is far too small to rule out other transport mechanisms, variable range hopping has been proposed as a conduction mechanism for manganites in the paramagnetic region [26–28]. VRH, however, cannot explain the unexpected path followed by the resistance during the first heating ramp. The initial deviation from VRH may be explained by the diffusion of oxygen vacancies towards the interface, as in the case of figure 2.

We repeated the experiment with setup #2, this time with temperature in a narrower range from 303 K to 373 K, varying with a rate of up to $\pm$ 6 K min^{-1}. Results are presented in figure 4. A qualitative similar behaviour is obtained: resistance deviates from the VRH prediction only during the first

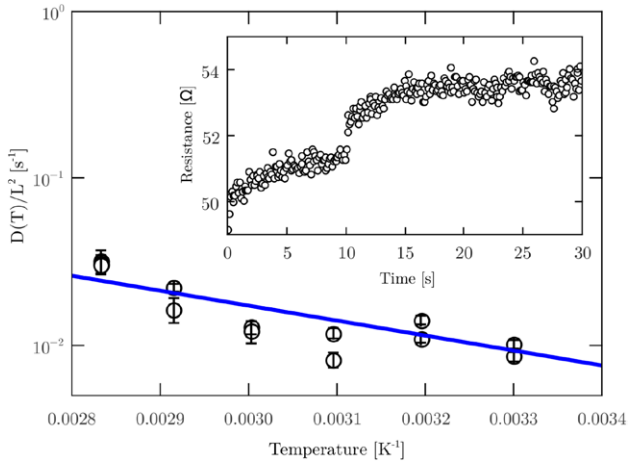

Figure 2. Diffusion coefficient as a function of temperature. The activation energy obtained is (0.18 ± 0.03) eV. Inset: time evolution of the HR state at 353 K. Two consecutive diffusion processes are observed at this temperature.

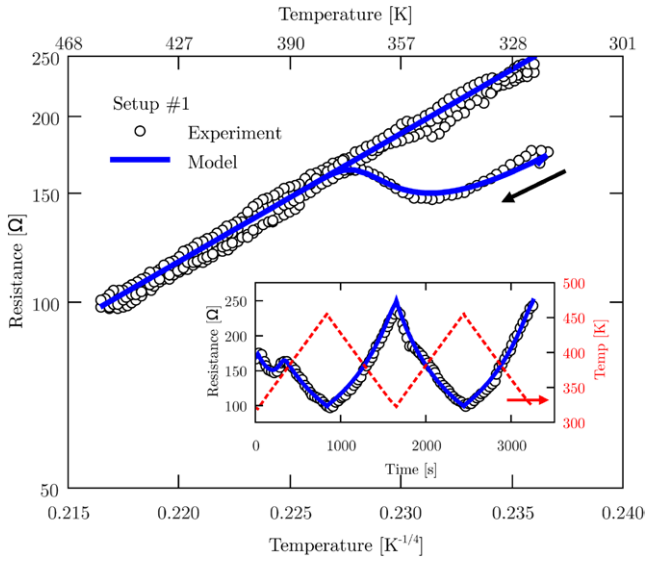

Figure 3. Experimental results for setup #1 showing the temperature behavior of the contact HR, $R_A(T)$. The arrow indicates the starting direction. At $T \gtrsim 373$ K the sample is fully diffused. The solid blue line is the model fit. Inset: time evolution of $R_A(T)$, model fit and temperature (red dashed-line). Temperature was swept from 323 K to 455 K at a rate of ± 10 K min^{-1} using a LakeShore 331 Temperature Controller.

temperature cycle. Again, we may find a qualitative explanation of the observed behaviour by assuming that oxygen vacancies continue pouring into a region close to the interface after the external stimulus has disappeared. Furthermore, Ov diffusion is alternatively activated or 'frozen' by either increasing or decreasing the temperature, respectively. Extending these ideas, in the following section we put forth a simplified quantitative Ov diffusion model that accounts well for the observations in figures 2–4.

3. Diffusion model

Based on the predictions of the VEOV model, our interpretation of the observed behaviour is the following: the negative polarity of the reset pulse forces oxygen vacancies to move from the bulk to the interface region, increasing its resistance R_A [12]. However, the Ov distribution is far from equilibrium because the reset pulse does not succeed in introducing vacancies homogeneously in all the interface and some nanoscale regions remain void of vacancies. After the reset pulse, the dynamics is governed by diffusion. At room temperature, the diffusion coefficient $D(T)$ for Ov is too small to effectively compensate for the density gradient obtained as a consequence of the reset pulse. As temperature is raised, $D(T)$ rapidly increases enabling former void regions to be infilled with vacancies, thus producing the concomitant increase in resistance. This process lasts until the steady configuration is attained. A picture of the proposed mechanism is shown in figure 1(*b*).

To be definite we proposed a very simplified 1D model of vacancy diffusion near the interface. Calling x to the spatial coordinate, we model the interface as the interval $-L < x < L$. We further assume that, after the reset pulse, Ov density n is constant everywhere but in a void region $(-x_o, +x_o)$,

$$n(x, t=0) = \begin{cases} 0 & x \in (-x_o, +x_o), \\ n_b & x \in (-L, -x_o] \cup [+x_o, +L), \end{cases} \tag{2}$$

t is the time. We do not expect the results to be qualitatively different for a different choice of $n(x, t = 0)$, as long as it contains a strong discontinuity. In addition the extension to the 2D and 3D is straightforward in Cartesian coordinates. Vacancy infilling dynamics are governed by Fick's second law,

$$\frac{\partial n}{\partial t} = D(T)\frac{\partial^2 n}{\partial x^2} \qquad x \in (-L, +L),\ t > 0. \tag{3}$$

The diffusion coefficient $D(T)$ is thermally activated with activation energy ϵ

$$D(T) = D_0 \exp\left(\frac{-\epsilon}{k_B T}\right), \tag{4}$$

where the prefactor D_0 is the diffusion coefficient at infinite T and k_B the Boltzmann constant.

Following the VEOV model assumption, we then consider a linear dependence between the value of R_0 in (1) and the total number of vacancies in the formerly void region,

$$R_0 \approx R_0' + B\int_{-x_o}^{+x_o} n(x, t)\,\mathrm{d}x, \tag{5}$$

where R'_0 and B are two arbitrary values.

Solving equations (1)–(5), we obtain that

$$R(t) \approx \left[R_0' + B\left(\frac{x_o}{L} - \sum_{k=1}^{\infty}\phi_k\psi(t)\right)\right]\exp\left(\frac{T_0}{T}\right)^{\frac{1}{4}}, \tag{6}$$

where

$$\phi_k = \left(\frac{\sqrt{2}\,\sin\left(k\pi\frac{x_o}{L}\right)}{k\pi}\right)^2, \tag{7}$$

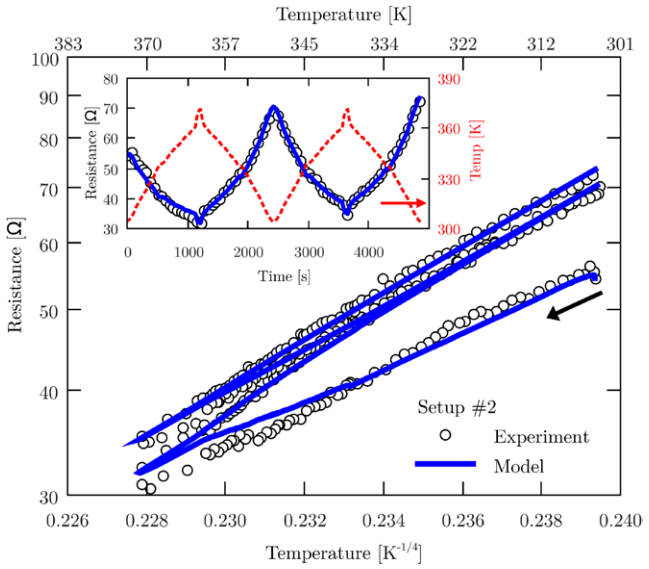

Figure 4. Experimental results for setup #2 showing the temperature behavior of the contact resistance $R_A(T)$. The arrow indicates the starting direction. The sample continues the diffusion process for more than one cycle. The solid blue line is the model fit. Inset: time evolution of $R_A(T)$, model fit and temperature (red dashed-line). Temperature was swept from 303 K to 373 K at a rate of up to ± 6 K min^{-1} by heating the sample with a Peltier cell controlled by an Arduino board.

$$\psi(t) = \exp\left\{-(k\pi)^2 \frac{D_0}{L^2} \int_0^t \exp\left(\frac{-\epsilon}{k_B T(t')}\right) dt'\right\}. \quad (8)$$

4. Model fit

We fit (6) to the experimental measurements of R_A (see figures 3–4). First, $T_0^{1/4}$ was obtained from stable regions in the experiments presented in figures 3 and 4, i.e. long after transients have passed. Fitted values of $T_0^{1/4}$ were in the range of [45, 57] K$^{1/4}$. These values are not far from those reported in [26]. Using (6), we then looked for the values of x_o/L, D_0/L^2 and ϵ which minimized the mean square error between the experimental results and simulated values. As it can be seen in figures 3–4, the simple model in section 3 fits experimental data well.

Among different experiments, we obtained $x_o/L \sim 0.5$. In the case of ϵ—the height of the barrier that maintains the system in a metastable out-of-equilibrium condition immediately after the writing pulse—we got values ranging between 0.2–1.3 eV. As a reference, Nian *et al* [15] estimated 0.4 eV for another manganite. Regarding the dispersion in the values, we hypothesize that it is evidencing a broad distribution of anchoring energies instead of the mono-energetic level considered in our model. Moreover, experimentally we have little control (if any) in the way this broad distribution of states is infilled.

Extracting D_0/L^2 is not straightforward because it is exponentially affected by the estimated value of ϵ. In fact, there is a strong nonlinear covariance between ϵ and D_0/L^2 in the proposed minimization method. Therefore, we estimated $D(T)/L^2$ from the measured time evolution of resistance for a fixed temperature and the first term in (6). In the inset of figure 2, we present an example of the evolution of the resistance after setting the HR state at 353 K. We hypothesize that the two successive exponential-like-increase intervals could correspond to the sequential infilling of two vacancy-void regions. Indeed, we also obtained good fits (not shown here) of figures 3–4 with a two-vacancy-void-region model. Figure 2 displays the results for six temperatures (two measurements for each temperature) together with the fit from which we extracted $\epsilon \sim 0.2$ eV, $D_0/L^2 \sim 90$ s^{-1}. A value of $D_0 \sim 2 \cdot 10^{-7}$ cm^2 s^{-1} is obtained by setting $L = 500$ nm, which is fully consistent with reported oxygen diffusion constant in perovskite-based oxides [15, 29].

5. Conclusions

By performing temperature sweeps of the high resistance state in a perovskite-based memristive interface, and relying on simple assumptions of the VEOV model, we extracted confident values of relevant parameters involved in the kinetics of Ov diffusion. We found that the electric pulse might set the system in a metastable configuration that relaxes after overcoming a barrier of 0.2—1.3 eV. In addition the estimated diffusion coefficient values for Ov are consistent with the literature. Our results support a switching dynamics consistent both with the VEOV model and the assumption of a linear relation between resistivity and Ov concentration in regions near the electrode interface [21].

Finally, the metastability here reported could be also further exploited in resistive switching binary memories, as it actually increases the resistance of the high resistance state (i.e. it improves the ON/OFF ratio).

Acknowledgments

This work was partially supported by CONICET (PIP 11220080101821), Agencia Nacional de Promoción Científica y Tecnológica (ANPCyT) (PICT-2010 # 121), Fundación Balseiro and ITBA (ITBACyT-2013 # 6). We acknowledge P Levy and G Leyva for providing the LPCMO samples, and for the use of facilities at GIA-CAC-CNEA, Argentina. PS acknowledges the Ramón y Cajal program (RYC-2012-01031). GAP and PIF acknowledge F Sangiuliano Jimka for lab assistance. The authors would like to thank M Rozenberg, F Gomez-Marlasca, N Ghenzi, C Acha and D F Grosz for useful discussions.

References

[1] Meijer G 2008 Materials science. Who wins the nonvolatile memory race? *Science* **319** 1625–6
[2] Sawa A 2008 Resistive switching in transition metal oxides *Mater. Today* **11** 28–36
[3] Ielmini D, Spiga S, Nardi F, Cagli C, Lamperti A, Cianci E and Fanciulli M 2011 Scaling analysis of submicrometer nickel-oxide-based resistive switching memory devices *J. Appl. Phys.* **109** 034506

[4] Liu Z J, Gan J Y and Yew T R 2012 ZnO-based one diode-one resistor device structure for crossbar memory applications *Appl. Phys. Lett.* **100** 153503
[5] Kugeler C, Rosezin R, Weng R, Waser R, Menzel S, Klopstra B and Bottger U 2009 Fast resistive switching in wo3 thin films for non-volatile memory applications *9th IEEE Conference on Nanotechnology (Genoa, 26–30 July)* pp 900–3
[6] Fujiwara K, Nemoto T, Rozenberg M J, Nakamura Y and Takagi H 2008 Resistance switching and formation of a conductive bridge in metal/binary oxide/metal structure for memory devices *Japan. J. Appl. Phys.* **47** 6266
[7] Ebrahim R, Wu N and Ignatiev A 2012 Multi-mode bipolar resistance switching in cuxo films *J. Appl. Phys.* **111** 034509
[8] Tsui S, Wang Y Q, Xue Y Y and Chu C W 2006 Mechanism and scalability in resistive switching of metal-$Pr_{(0.7)}Ca_{(0.3)}MnO_{(3)}$ interface *Appl. Phys. Lett.* **89** 123502
[9] Szot K, Speier W, Bihlmayer G and Waser R 2006 Switching the electrical resistance of individual dislocations in single-crystalline $SrTiO_{(3)}$ *Nat. Mater.* **5** 312–20
[10] Janousch M, Meijer G, Staub U, Delley B, Karg S and Andreasson B 2007 Role of oxygen vacancies in cr-doped $SrTiO_{(3)}$ for resistance-change memory *Adv. Mater.* **19** 2232–5
[11] Quintero M, Levy P, Leyva A G and Rozenberg M J 2007 Mechanism of electric-pulse-induced resistance switching in manganites *Phys. Rev. Lett.* **98** 116601
[12] Gomez-Marlasca F, Ghenzi N, Stoliar P, Sánchez M J, Rozenberg M J, Leyva G and Levy P 2011 Asymmetric pulsing for reliable operation of titanium/manganite memristors *Appl. Phys. Lett.* **98** 123502
[13] Ghenzi N, Sánchez M J, Rozenberg M J, Stoliar P, Marlasca F G, Rubi D and Levy P 2012 Optimization of resistive switching performance of metal-manganite oxide interfaces by a multipulse protocol *J. Appl. Phys.* **111** 084512
[14] Stoliar P, Levy P, Sánchez M, Leyva A, Albornoz C, Gomez-Marlasca F, Zanini A, Toro Salazar C, Ghenzi N and Rozenberg M 2014 Nonvolatile multilevel resistive switching memory cell: a transition metal oxide-based circuit *IEEE Trans. Circuits Syst. II: Express Briefs* **61** 21–5
[15] Nian Y B, Strozier J, Wu N J, Chen X and Ignatiev A 2007 Evidence for an oxygen diffusion model for the electric pulse induced resistance change effect in transition-metal oxides *Phys. Rev. Lett.* **98** 146403
[16] Chen S-C, Chang T-C, Chen S-Y, Chen C-W, Chen S C, Sze S M, Tsai M-J, Kao M-J and Yeh F S 2011 Bipolar resistive switching of chromium oxide for resistive random access memory *Solid-State Electron.* **62** 40–3
[17] Wang Z H, Yang Y, Gu L, Habermeier H U, Yu R C, Zhao T Y, Sun J R and Shen B G 2012 Correlation between evolution of resistive switching and oxygen vacancy configuration in $La_{(0.5)}Ca_{(0.5)}MnO_{(3)}$ based memristive devices *Nanotechnology* **23** 265202
[18] Liu Z, Zhang P, Meng Y, Tian H, Li J, Pan X, Liang X, Chen D and Zhao H 2012 Effect of taox thickness on the resistive switching of Ta/$Pr_{(0.7)}Ca_{(0.3)}MnO_{(3)}$/Pt films *Appl. Phys. Lett.* **100** 143506
[19] Zazpe R, Stoliar P, Golmar F, Llopis R, Casanova F and Hueso L E 2013 Resistive switching in rectifying interfaces of metal-semiconductor-metal structures *Appl. Phys. Lett.* **103** 073114
[20] Jung C H, Park M K and Woo S I 2012 Improvement of oxygen vacancy migration through nb doping on $Ba_{(0.7)}Sr_{(0.3)}TiO_{(3)}$ thin films for resistance switching random access memory application *Appl. Phys. Lett.* **100** 262107
[21] Rozenberg M J, Sánchez M J, Weht R, Acha C, Gomez-Marlasca F and Levy P 2010 Mechanism for bipolar resistive switching in transition-metal oxides *Phys. Rev.* B **81** 115101
[22] Ghenzi N, Sánchez M J, Gomez-Marlasca F, Levy P and Rozenberg M J 2010 Hysteresis switching loops in ag-manganite memristive interfaces *J. Appl. Phys.* **107** 093719
[23] Levy P, Parisi F, Quintero M, Granja L, Curiale J, Sacanell J, Leyva G, Polla G, Freitas R S and Ghivelder L 2002 Nonvolatile magnetoresistive memory in phase separated $La_{(0.325)}Pr_{(0.300)}Ca_{(0.375)}MnO_{(3)}$ *Phys. Rev.* B **65** 140401
[24] Patterson G A, Fierens P I and Grosz D F 2013 On the beneficial role of noise in resistive switching *Appl. Phys. Lett.* **103** 074102
[25] Ambegaokar V, Halperin B I and Langer J S 1971 Hopping conductivity in disordered systems *Phys. Rev.* B **4** 2612–20
[26] Viret M, Ranno L and Coey J M D 1997 Colossal magnetoresistance of the variable range hopping regime in the manganites *J. Appl. Phys.* **81** 4964–6
[27] Viret M, Ranno L and Coey J M D 1997 Magnetic localization in mixed-valence manganites *Phys. Rev.* B **55** 8067–70
[28] Sun Y, Xu X and Zhang Y 2000 Variable-range hopping of small polarons in mixed-valence manganites *J. Phys.: Condens. Matter* **12** 10475
[29] Watterud G 2005 Determination of oxygen transport coefficients in perovskites, perovskite related materials with mixed conductivity *PhD thesis* Norwegian University of Science and Technology (www.diva-portal.org/smash/get/diva2:125879/FULLTEXT01.pdf)